

Antibacterial activity and mechanism of silver nanoparticles on *Escherichia coli*

Wen-Ru Li · Xiao-Bao Xie · Qing-Shan Shi ·
Hai-Yan Zeng · You-Sheng OU-Yang · Yi-Ben Chen

Received: 11 June 2009 / Revised: 8 July 2009 / Accepted: 18 July 2009 / Published online: 11 August 2009
© Springer-Verlag 2009

Abstract The antibacterial activity and acting mechanism of silver nanoparticles (SNPs) on *Escherichia coli* ATCC 8739 were investigated in this study by analyzing the growth, permeability, and morphology of the bacterial cells following treatment with SNPs. The experimental results indicated 10 µg/ml SNPs could completely inhibit the growth of 10⁷ cfu/ml *E. coli* cells in liquid Mueller–Hinton medium. Meanwhile, SNPs resulted in the leakage of reducing sugars and proteins and induced the respiratory chain dehydrogenases into inactive state, suggesting that SNPs were able to destroy the permeability of the bacterial membranes. When the cells of *E. coli* were exposed to 50 µg/ml SNPs, many pits and gaps were observed in bacterial cells by transmission electron microscopy and scanning electron microscopy, and the cell membrane was fragmentary, indicating the bacterial cells were damaged severely. After being exposed to 10 µg/ml SNPs, the membrane vesicles were dissolved and dispersed, and their membrane components became disorganized and scattered from their original ordered and close arrangement based on TEM observation. In conclusion, the combined results suggested that SNPs may damage the structure of bacterial cell membrane and depress the activity of some membranous enzymes, which cause *E. coli* bacteria to die eventually.

Keywords Silver nanoparticles (SNPs) · *Escherichia coli* · Antibacterial mechanism · Permeability · Bacterial membrane

Introduction

It has been known that silver and its compounds have strong inhibitory and bactericidal effects as well as a broad spectrum of antimicrobial activities for bacteria, fungi, and virus since ancient times (Lok et al. 2006; Cho et al. 2005; Silver 2003). Compared with other metals, silver exhibits higher toxicity to microorganisms while it exhibits lower toxicity to mammalian cells (Zhao and Stevens 1998). Nanometer-sized silver particles have been known for a long time but have been paid little attention (Lok et al. 2006). Lately, the recent advances in researches on metal nanoparticles appear to revive the use of silver nanoparticles (SNPs) for antimicrobial applications. It has been shown that SNPs prepared with a variety of synthetic methods have effective antimicrobial activity (Lok et al. 2006; Baker et al. 2005; Aymonier et al. 2002; Melaiye et al. 2005; Sondi and Salopek-Sondi 2004; Kim et al. 2008a, b; Lee et al. 2008; Alt et al. 2004). Hence, SNPs have been applied to a wide range of healthcare products, such as burn dressings, scaffold, water purification systems, and medical devices (Thomas et al. 2007; Kim and Kim 2006).

The toxic effects of silver on bacteria have been investigated for more than 60 years (Franke et al. 2001). And the acting mechanism of silver has been known in some extent (Rai et al. 2009). Ag⁺ inhibits phosphate uptake and exchange in *Escherichia coli* and causes efflux of accumulated phosphate as well as of mannitol, succinate, glutamine, and proline (Schreurs and Rosenberg 1982). Moreover, Dibrov et al. demonstrated that Ag⁺ carried the ability to collapse the proton motive force of *Vibrio*

W.-R. Li · X.-B. Xie (✉) · Q.-S. Shi · H.-Y. Zeng ·
Y.-S. OU-Yang (✉) · Y.-B. Chen
Guangdong Institute of Microbiology,
Guangzhou 510070, China
e-mail: xxiaobao@tom.com
e-mail: ouyang6411@21cn.com

W.-R. Li · X.-B. Xie · Q.-S. Shi · H.-Y. Zeng · Y.-S. OU-Yang ·
Y.-B. Chen
Guangdong Provincial Key Laboratory of Microbial Culture
Collection and Application,
Guangzhou 510070, China

cholera. Considering the well-documented crucial importance of the transmembrane proton gradient in overall microbial metabolism, it seems inevitable that the elimination of proton motive force should result in cell death (Dibrov et al. 2002). Ag^+ also forms complexes with bases contained in DNA and is a potent inhibitor of fungal DNAases (Ahearn et al. 1995; Ghandour et al. 1988). Moreover, Ag^+ can lead to enzyme inactivation via formatting silver complexes with electron donors containing sulfur, oxygen, or nitrogen (thiols, carboxylates, phosphates, hydroxyl, amines, imidazoles, indoles; Ahearn et al. 1995). Ag^+ may displace native metal cations from their usual binding sites in enzymes (Ghandour et al. 1988). Furthermore, silver ions inhibit oxidation of glucose, glycerol, fumarate, and succinate in *E. coli* (Ahearn et al. 1995).

Though the mode of action of SNPs on the bacteria is still unknown, its possible mechanism of action has been suggested according to the morphological and structural changes in the bacterial cells (Rai et al. 2009). The SNPs show efficient antimicrobial property compared with other salts due to their extremely large surface area, which provides better contact with microorganisms (Rai et al. 2009). For *E. coli* cells, a short time of exposure to antibacterial concentrations of SNPs resulted in an accumulation of envelope protein precursors. This indicates that SNPs may target at the bacterial membrane, leading to a dissipation of the proton motive force (Lok et al. 2006). When silver nanoparticles enter the bacterial cell, they form a low molecular weight region inside the bacteria. Thus, the bacteria conglomerate to protect the DNA from the SNPs. Consequently, the nanoparticles preferably attack the respiratory chain, cell division finally leading to cell death (Rai et al. 2009).

In this paper, to understand the antibacterial activity and acting mechanism of SNPs deeply, we studied the mechanism of inhibition to *E. coli* by SNPs in the cellular and subcellular levels. For the first time, we offer evidences to indicate that SNPs can inhibit bacterial growth and even kill the cells through destroying bacterial membranous structure and permeability.

Materials and methods

Reagents

SNPs solutions AGS-WMB1000C were purchased from Shanghai Huzheng Nanotechnology Company limited (Shanghai, China). The average diameter size of Ag particles is 5 nm, and Ag content density is 1,000 ppm. The sizes and morphology of nano-Ag were examined using a transmission electron microscope (JEOL JEM-2010HR), and the elemental analysis was examined by energy dispersive X-ray spectroscopy (EDX; Oxford ISIS-300; Fig. 1). Iodonitrotetrazolium chloride (INT) reagent for respiration measurement was purchased from Fluka Chemie GmbH Company (Buchs Switzerland).

Organism, medium, and cultivation

The strain of *E. coli* ATCC8739 was purchased from American Type Culture Collection (ATCC) and conserved in our laboratory. Mueller–Hinton (MH) medium (purchased from Guangdong Huankai Microbial Sci. and Tech. Co., Ltd, Guangzhou, China; final pH 7.3 ± 0.2) contains the following: 2.0 g beef extract, 1.5 g soluble starch, and 17.5 g acid hydrolysate of casein. MH medium was used

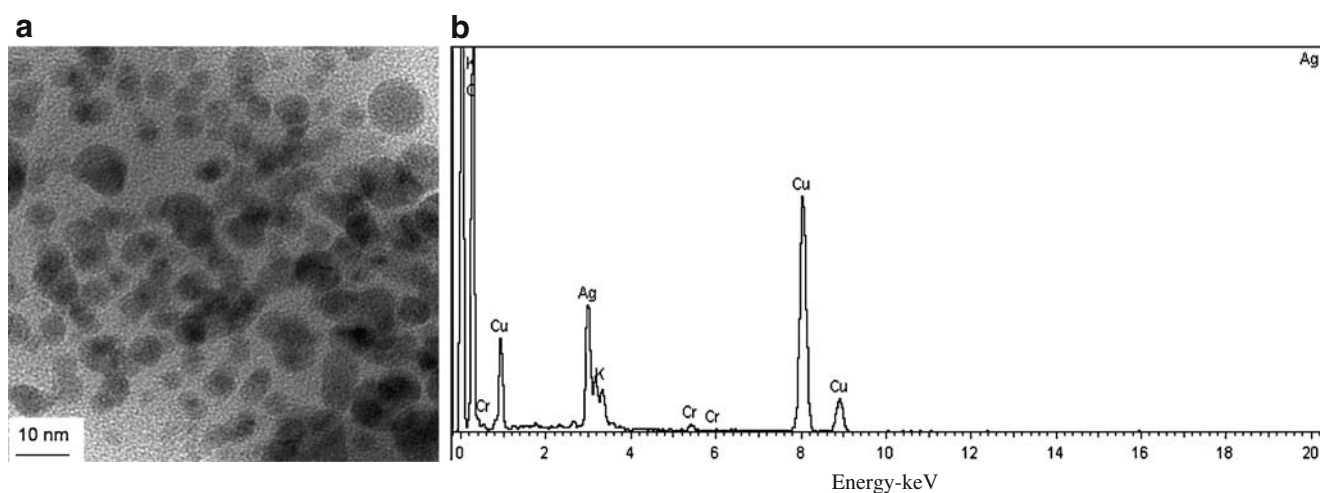


Fig. 1 Size and morphology elemental analysis of SNPs by TEM (a) and EDX (b)

for aerobic cultivation at 37°C with shaking at 150 rpm. Growth curves of *E. coli* exposed and unexposed to SNPs were determined based on the absorbing value of OD₆₀₀.

Assay for minimum inhibitory concentration of SNPs

To examine the minimum inhibitory concentration of SNPs and the growth curves of *E. coli* exposed to SNPs, different volume of MH medium, SNPs solutions, and *E. coli* cells were added separately to 20 ml cultures in five conical flasks (50 ml), resulting in final concentrations of SNPs of 0, 1.25, 2.5, 5, and 10 µg/ml, respectively, and concentration of 10⁷ cfu/ml *E. coli* cells. The cultures were incubated at 37±2°C and shaken at 150 rpm. Growth rates and bacterial concentrations were determined by measuring optical density (OD) at 600 nm (0.1 OD₆₀₀ corresponding to 10⁸ cells per milliliter) through time series.

Assay about the effect of SNPs on leakage of the membrane in *E. coli*

To detect the leakage of reducing sugars and proteins through membrane, different volumes of MH medium, SNPs, and *E. coli* cells were added into 10 ml cultures with final concentration of 100 µg/ml SNPs and 10⁹ cfu/ml *E. coli*. Control experiments were conducted without SNPs. The cultures were incubated at 37±2°C with shaking at 150 rpm. One milliliter culture was sampled from the cultures when SNPs were added into cultures and after being treated for 2 or 4 h. The sample was centrifuged at 12,000 rpm, the supernatant liquid was frozen at -30°C immediately, and then the concentrations of reducing sugars and proteins were determined as soon as possible (Bradford 1976; Miller 1959).

Assay about the effect of SNPs on enzymatic activity of respiratory chain dehydrogenases in *E. coli*

The dehydrogenase activity was determined according to previous iodionitrotetrazolium chloride method (Iturriaga et al. 2001; Kim et al. 1994, 2009) with slight modification. Under physiological conditions, colorless INT is reduced by the bacterial respiratory chain dehydrogenase to a dark-red water-insoluble iodionitrotetrazolium formazan (INF); thus, the dehydrogenase activity can be determined by the change of the spectrophotometric value of INF. Different volumes of MH medium and nanosilver, *E. coli* cells were added into 10 ml cultures separately resulting in final concentrations of nanosilver at 10 and 50 µg/ml and final concentrations of 10⁸ cfu/ml *E. coli*. Experiments were conducted in absence of SNPs as the control. The *E. coli* cells were boiled for 20 min to inactivate the enzymes completely as the control (-), while the cells were not boiled, and their enzymes maintained native activity as the

control (+). Cultivations were performed at 37±2°C with shaking at 150 rpm. One milliliter culture was sampled separately from the cultures and centrifuged at 12,000 rpm, then the supernatants were discarded and the bacteria washed by phosphate-buffered saline (PBS) twice and added 0.9 ml PBS to suspend the bacteria. INT solution (0.1 ml 0.5%) was added, the culture was incubated at 37°C in dark for 2 h, and then 50 µl formaldehyde was added to terminate the reaction. The culture was centrifuged to collect the bacteria, and 250 µl solutions of acetone and ethanol 1:1 in volume were used to distill the INF twice. The supernatants were finally combined. The dehydrogenase activity was then calculated according to the maximum spectrophotometrical absorbance of INF at 490 nm by spectrophotometer (DU640, Beckman).

Observation of the action of SNPs on the membrane structure of *E. coli*

Different volume of MH medium, SNPs solutions, and *E. coli* cells were added to 10 ml cultures resulting in final concentration of 50 µg/ml and concentration of 10⁸ cfu/ml *E. coli*. Control experiment was conducted in absence of SNPs. The cultures were incubated at 37±2°C with shaking at 150 rpm for 12 h. The cultures were centrifuged and the supernatants discarded for observation by transmission electron microscopy (TEM, Hitachi H-7650) and scanning electron microscopy (SEM, Hitachi S-3000N).

Observation of the action of SNPs on the membrane vesicles structure of *E. coli*

The membrane isolation and vesicle preparation were performed using the method of Sapra et al. (2003) with some modifications. Buffer A [50 mM Tris-HCl buffer (pH 8.0) containing 2 mM sodium dithionite] was employed throughout. The cell-free extracts of *E. coli* were prepared by suspending 5 g (wet weight) of frozen cells in 50 ml buffer A. The cell suspensions were then sonicated in an ice bath (3 s, 40% output, 80× SONICS VC-505; USA), and the cell breakage was monitored by examining the cells with a microscope. The unbroken cells were removed by centrifugation at 10,000 rpm for 15 min, and the crude extract was centrifuged at 40,000 rpm for 2 h. The resulting pellets contained the cell membranes, whereas the cytoplasmic proteins remained in the supernatants. The membrane fractions were resuspended in buffer A to allow the spontaneous formation of vesicles, which were confirmed by TEM. Fifty milliliters of membrane vesicles was treated with 10 µg/ml nanosilver for 2 h, and control experiment was conducted in absence of nanosilver. The membrane vesicles (MVs) exposed and unexposed to SNPs were observed via TEM.

Results

Growth curve of *E. coli* exposed to SNPs

The growth curves of *E. coli* treated with SNPs were shown in Fig. 2 by measuring optical density at 600 nm. In presence of 0, 1.25, 2.5, and 5 $\mu\text{g/ml}$ of SNPs, the growth curves of *E. coli* included three phases: lag phase, exponential phase, and stabilization phase. However, decline phases in each growth curve could not be revealed because we only assayed the total numbers of bacteria, including live and dead ones, based on the value of OD_{600} . Under absence of SNPs, *E. coli* reached exponential phase rapidly. But exposed to 1.25, 2.5, and 5 $\mu\text{g/ml}$ of SNPs, *E. coli* cells were lagged to 12, 36, and 48 h, respectively. With the increasing concentration of SNPs, the delay was more evident. When the concentration of SNPs was 10 $\mu\text{g/ml}$, no growth of *E. coli* could be detected within 7 days, indicating the minimum inhibitory concentration (MIC) of SNPs to *E. coli* was 10 $\mu\text{g/ml}$.

Effect of SNPs on the membrane leakage of reducing sugars and proteins

Figure 3a revealed that SNPs could enhance the membrane leakage of reducing sugars. In starting time, almost no reducing sugars could be detected to leak from bacterial cells in control experiment, while the leakage amount of reducing sugars from cells treated with SNPs was 27.5 μg per bacterial dry weight of 1 mg ($\mu\text{g/mg}$). After treatment with SNPs for 2 h, the leakage amount of reducing sugars was up to 102.5 μg per bacterial dry weight of 1 mg, but there was only 30 $\mu\text{g/mg}$ in control experiment, suggesting SNPs may accelerate the reducing sugars leakage from bacterial cytoplasm.

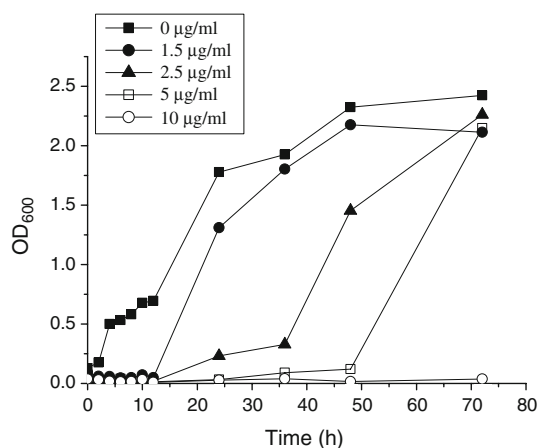


Fig. 2 Growth curves of *E. coli* cells exposed to different concentrations of SNPs

Similarly, SNPs also elevated the leakage of proteins through the membrane of *E. coli* (Fig. 3b). In starting time, the leakage of proteins from cells in control experiment was 5.89 $\mu\text{g/mg}$, while leakage of proteins from cells treated with SNPs was 6.56 $\mu\text{g/mg}$. The leakage of proteins in *E. coli* treated with SNPs for 4 h was up to 11.96 $\mu\text{g/mg}$, which enhanced 57% that in control experiment (7.61 $\mu\text{g/mg}$).

Effect of SNPs on respiratory chain dehydrogenases of *E. coli*

The effect of SNPs on respiration chain dehydrogenases of *E. coli* was shown in Fig. 4. Activity of respiratory chain dehydrogenases in control (+) cells increased with the incubation time, while the activity of respiratory chain dehydrogenases has nearly no change in the control (–) cells of the *E. coli* boiled for 20 min. Interestingly, enzymatic activity of cells treated with 5 $\mu\text{g/ml}$ SNPs was even higher than that of control (+) in initial time, but its activity fell down rapidly with increase of incubating time. After being treated for 10 min with 5 $\mu\text{g/ml}$ SNPs, the enzymatic activity almost fell to the bottom, maintaining feeble activity during treatment for 30 min. Enzymatic activity of cells treated with 50 $\mu\text{g/ml}$ SNPs was always very lower than that of cells treated with 5 $\mu\text{g/ml}$ SNPs. The results indicated that the activity of respiratory chain dehydrogenases of *E. coli* could be inhibited by SNPs, and the higher concentration of SNPs, the lower the activity of enzymes.

Action of SNPs on the structures of *E. coli* cells

The electron micrographs by SEM and TEM of *E. coli* cells treated and untreated with SNPs were displayed in Fig. 5. Micrograph by SEM (Fig. 5a) showed the surface of *E. coli* cells untreated with SNPs was smooth and showed typical characters of rod shape, while cells treated with 50 $\mu\text{g/ml}$ SNPs (Fig. 5b) were damaged severely. Some cells showed large leakage, others misshapen and fragmentary. Micrographs by TEM (Fig. 5c, d) showed the surface of native cells was smooth and intact, and some filaments around cells were obvious and clear which were peritrichous flagella of *E. coli* cells, while membrane of treated cells were damaged severely; many pits and gaps appeared in the micrograph, and their membrane was fragmentary. In addition, electron-dense particles or precipitates were also observed around damaged bacterial cells.

Action of SNPs on the membrane vesicle structures of *E. coli*

Membrane fragments of *E. coli* could form vesicles spontaneously in buffer A. The vesicles resembled the spheroid. Their diameters were between 25 and 250 nm,

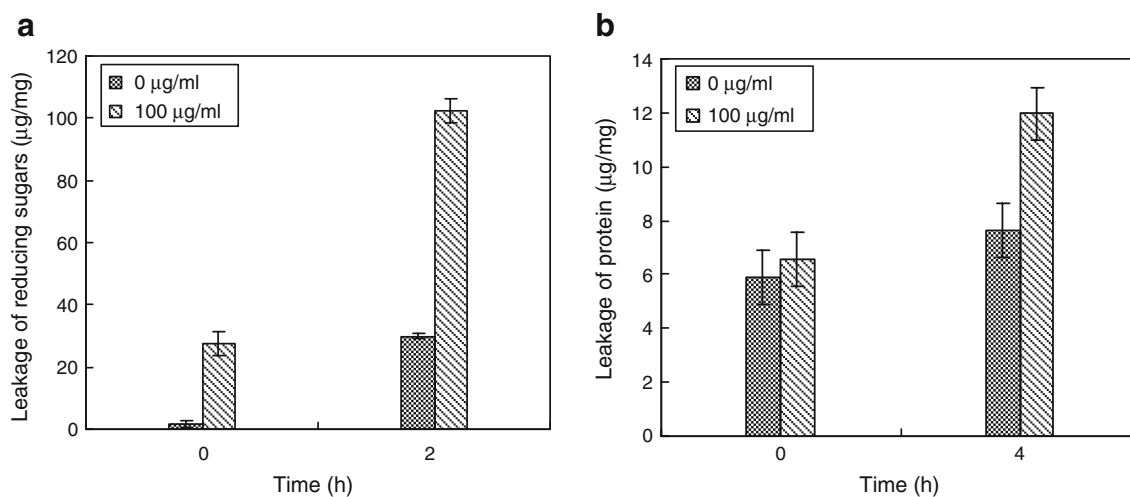


Fig. 3 Leakage of reducing sugars (a) and proteins (b) from *E. coli* cells treated with SNPs. Data are average from duplicate experiments. Error bars represent standard deviations of duplicate incubations

and their sizes were between 1/20 and 1/5 of the *E. coli* cells. The vesicles were empty without internal structure. After being treated with SNPs, MVs were dissolved and dispersed. Their membrane components became disorganized and scattered from their original ordered and close arrangement. But in the controls untreated with SNPs, the electron micrograph of MVs showed they were intact and clear-cut (Fig. 6).

Discussion

The growth curves of *E. coli* exposed to SNPs indicated that SNPs could inhibit the growth and reproduction of *E. coli*. A minor amount of SNPs could prolong the lag phase of *E. coli*. Until the concentration of SNPs was up to 10 µg/ml, *E.*

coli cells of 10^7 cfu/ml were completely inhibited, and then the MIC of SNPs was 10 µg/ml in this condition. According to this, the SNPs have perfect antibacterial activity.

To understand the antibacterial mechanism of SNPs to Gram-negative bacteria, we selected *E. coli* as model to study the effect of SNPs on the permeability and the membrane structure of *E. coli* cells. It is well known that Gram-negative bacteria possess an outer membrane outside the peptidoglycan layer lacking in Gram-positive organisms. The essential function of the outer membrane is to serve as a selective permeability barrier, protecting bacteria from harmful agents, such as detergents, drugs, toxins, and degradative enzymes, and penetrating nutrients to sustain bacterial growth. The structure and chemical composition of the outer membrane in *E. coli* cells has been studied extensively. The lipid bilayer of outer membrane is asymmetric: the inner leaflet mostly contains close-packed phospholipid chains, while the outer leaflet is composed of the lipopolysaccharide (LPS) molecules. It has been estimated that approximately 3.5 million molecules of LPS cover three quarters of the surface of *E. coli*, with the remaining quarter composed of membrane proteins. Evidence from genetic and chemical experiments have proved that the LPS layer of the outer membrane plays an essential role in providing a selective permeability barrier for *E. coli* and other Gram-negative bacteria. And mutant-altered LPS structures could increase permeability compared with that of native cells (Amro et al. 2000). Our experimental results showed that SNPs apparently enhanced the permeability of membrane for reducing sugars and proteins in cells. So it could be conferred that turbulence of membranous permeability would be an important factor to inhibit the bacterial growth. But it is still a mystery where the damage takes place, on the lipopolysaccharide or membrane proteins in outer membrane.

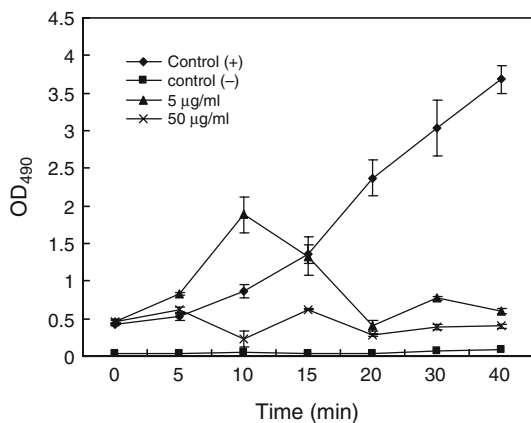


Fig. 4 Effect of SNPs on respiration chain dehydrogenases in *E. coli* cells. Data are average from duplicate experiments. Error bars represent standard deviations of duplicate incubations. The control (-) and control (+) represent the boiled and not boiled *E. coli* cells, respectively

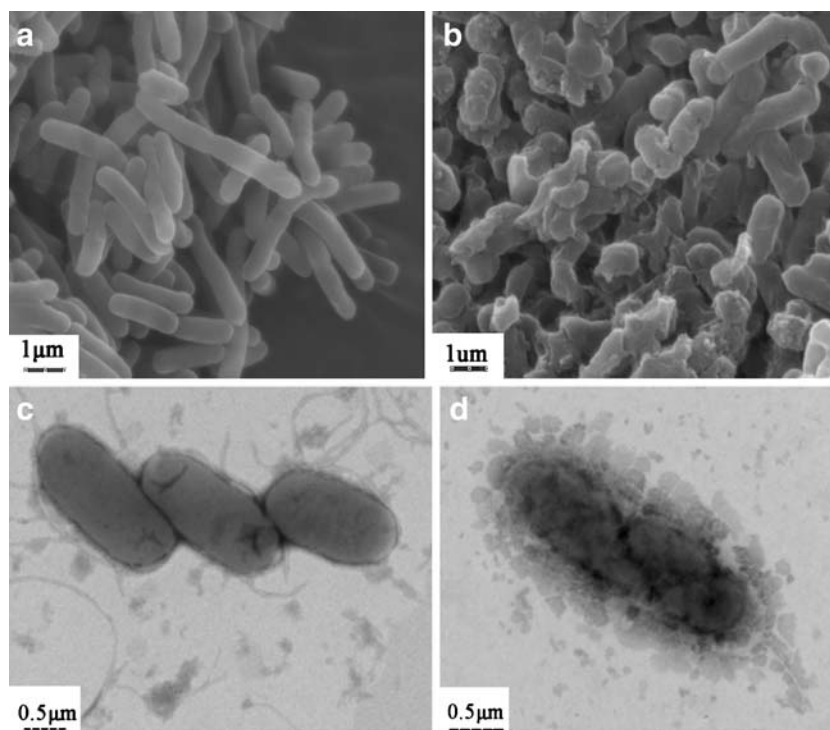


Fig. 5 Action of SNPs on *E. coli* cells observed by SEM (a, b) and TEM (c, d). a, c Cell structure of native *E. coli* cells; b, d cell structure of *E. coli* cells treated with 50 μg/ml SNPs

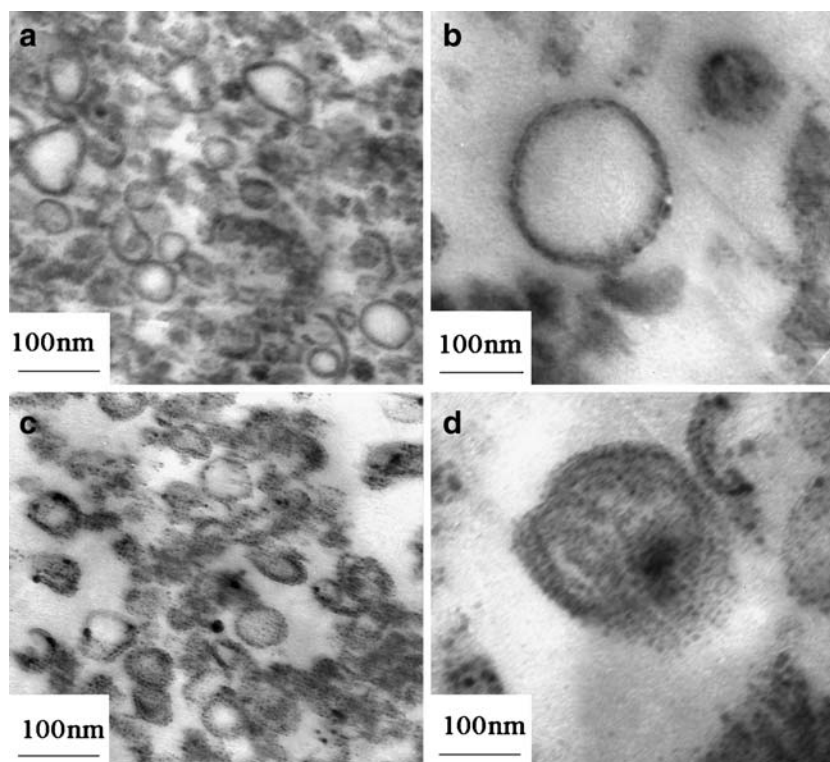


Fig. 6 Action of SNPs on membrane vesicles of *E. coli* cells observed by TEM. a, b Structure of native cell membrane vesicles; c, d structure of cell membrane vesicles treated with 10 μg/ml SNPs

Additionally, our results of experiments showed that the activity of respiratory chain dehydrogenases in *E. coli* might be inhibited by SNPs; the higher concentration of SNPs, the lower the activity of enzymes. It is assumed that SNPs may break through barrier of outer membrane permeability, peptidoglycan and periplasm, and destroy respiratory chain dehydrogenases, furthermore inhibiting respiration of cells. In 2005, Holt and Bard found that Ag^+ inhibited respiration of *E. coli* by determining change of oxygen dissolved in culture resolution (Holt and Bard 2005). Besides, Kim et al. found that Ag^+ interacted with thiol (–SH) group of cysteine by replacing the hydrogen atom to form –S–Ag, thus hindering the enzymatic function of affected protein to inhibit growth of *E. coli* (Kim et al. 2008a, b). However, the interaction between SNPs and enzymes still needs to be studied deeply.

From the TEM of MVs, we found the MVs treated with SNPs were dissolved and dispersed, and their membrane components became disorganized and scattered from their original ordered and close arrangement. Cell membrane was disaggregated and lost their intrinsic function. The TEM micrograph of *E. coli* cells treated with SNPs showed that big gaps appeared in the cell membrane, and the bacteria were almost disorganized to several parts. SEM micrograph of *E. coli* cells treated with SNPs showed many fragmentary bacteria. These phenomena suggest possible antibacterial mechanisms by which SNPs inhibit bacterial growth, as well as cellular responses to the SNP treatment.

Based on the present research, the action model of SNPs may be described as SNPs making a break through the permeability of outer membrane firstly, resulting in the leakage of cellular materials. Secondly, SNPs enter the inner membrane and inactivate respiratory chain dehydrogenases, thus inhibiting respiration and growth of cells. Simultaneously, SNPs could affect some proteins and phosphate lipids and induce collapse of membrane, resulting in cell decomposition and death eventually. Taking into account the mobility of SNPs into cells and their fate in a bioprocess or even in the environment, the risk aspects for the application in larger scales and in the environment should be strengthened in future study.

Acknowledgments This research was supported by Young People's Foundation of Guangdong Academy of Sciences (qj200806), Foundation of Enterprise-University-Research Institute Cooperation from Guangdong Province and Ministry of Education of China (2007B090400105 and 2008A010500005).

References

- Aheam DG, May LL, Gabriel MM (1995) Adherence of organisms to silver-coated surfaces. *J Ind Microbiol* 15:372–376
- Alt V, Bechert T, Steinrucke P, Wagener M, Seidel P, Dingeldein E, Domann E, Schnettler R (2004) An in vitro assessment of the antibacterial properties and cytotoxicity of nanoparticulate silver bone cement. *Biomaterials* 25:4383–4391
- Amro NA, Kotra LP, Wadu-Mesthrige K, Bulychev A, Mobashery S, Liu G (2000) High-resolution atomic force microscopy studies of the *Escherichia coli* outer membrane: structural basis for permeability. *Langmuir* 16:2789–2796
- Aymonier C, Schlotterbeck U, Antonietti L, Zacharias P, Thomann R, Tiller JC, Mecking S (2002) Hybrids of silver nanoparticles with amphiphilic hyperbranched macromolecules exhibiting antimicrobial properties. *Chem Commun* 24:3018–3019
- Baker C, Pradhan A, Pakstis L, Pochan DJ, Shah SI (2005) Synthesis and antibacterial properties of silver nanoparticles. *J Nanosci Nanotechnol* 5:244–249
- Bradford M (1976) A rapid and sensitive method for the quantitation of microgram quantities of protein utilizing the principle of protein-dye binding. *Analytical Biochem* 72:248–254
- Cho KH, Park JE, Osaka T, Park SG (2005) The study of antimicrobial activity and preservative effects of nanosilver ingredient. *Electrochim Acta* 51:956–960
- Dibrov P, Dzioba J, Gosink KK, Häse CC (2002) Chemiosmotic mechanism of antimicrobial activity of Ag^+ in *Vibrio cholerae*. *Antimicrob Agents Chemother* 46:2668–2670
- Franke S, Grass G, Nies DH (2001) The product of the ybdE gene of the *Escherichia coli* chromosome is involved in detoxification of silver ions. *Microbiol* 147:965–972
- Ghandour W, Hubbard JA, Deistung J, Hughes MN, Poole RK (1988) The uptake of silver ions by *Escherichia coli* K12: toxic effects and interaction with copper ion. *Appl Microbiol Biotechnol* 28:559–565
- Holt KB, Bard AJ (2005) Interaction of silver (I) ions with the respiratory chain of *Escherichia coli*: an electrochemical and scanning electrochemical microscopy study of the antimicrobial mechanism of micromolar Ag^+ . *Biochem* 44:13214–13223
- Iturriaga R, Zhang S, Sonek GJ, Stibbs H (2001) Detection of respiratory enzyme activity in *Giardia* cysts and *Cryptosporidium* oocysts using redox dyes and immunofluorescence techniques. *J Microbiol Methods* 46:19–28
- Kim S, Kim HJ (2006) Anti-bacterial performance of colloidal silver-treated laminate wood flooring. *Int Biodeterioration Biodegradation* 57:155–162
- Kim CW, Koopman B, Bitton B (1994) INT dehydrogenases activity test for assessing chlorine an dehydrogen peroxide inhibition of filamentous pure cultures and activated sludge. *Water Res* 28:1117–1121
- Kim KJ, Sung WS, Moon SK, Choi JS, Kim JG, Lee DG (2008a) Antifungal effect of silver nanoparticles on dermatophytes. *J Microbiol Biotechnol* 18(8):1482–1484
- Kim JY, Lee C, Cho M, Yoon J (2008b) Enhanced inactivation of *E. coli* and MS-2 phage by silver ions combined with UV-A and visible light irradiation. *Water Res* 42:356–362
- Kim KJ, Sung WS, Suh BK, Moon SK, Choi JS, Kim JG, Lee DG (2009) Antifungal activity and mode of action of silver nanoparticles on *Candida albicans*. *Biometals* 22:235–242
- Lee BU, Yun SH, Ji JH, Bae GN (2008) Inactivation of *S. epidermidis*, *B. subtilis*, and *E. coli* bacteria bioaerosols deposited on a filter utilizing airborne silver nanoparticles. *J Microbiol Biotechnol* 18:176–182
- Lok CN, Ho CM, Chen R, He QY, Yu WY, Sun H, Tam PK, Chiu JF, Chen CM (2006) Proteomic analysis of the mode of antibacterial action of silver nanoparticles. *J Proteome Res* 5:916–924
- Melaiye A, Sun Z, Hindi K, Milsted A, Ely D, Reneker DH, Tessier CA, Youngs WJ (2005) Silver(I)-imidazole cyclophane gem-diol complexes encapsulated by electrospun tectophilic nanofibers: formation of nanosilver particles and antimicrobial activity. *J Am Chem Soc* 127:2285–2291
- Miller G (1959) Use of dinitrosalicylic acid reagent for determination of reducing sugars. *Anal Chem* 31:426–429

- Rai M, Yadav A, Gade A (2009) Silver nanoparticles as a new generation of microbials. *Biotechnol Adv* 27:76–83
- Sapra R, Bagramyan K, Adams MWW (2003) A simple energy-conserving system: proton reduction coupled to proton translocation. *Proc Natl Acad Sci U S A* 100:7545–7550
- Schreurs WJA, Rosenberg H (1982) Effect of silver ions on transport and retention of phosphate by *Escherichia coli*. *J Bacteriol* 152:7–13
- Silver S (2003) Bacterial silver resistance: molecular biology and uses and misuses of silver compounds. *FEMS Microbiol Rev* 27:341–353
- Sondi I, Salopek-Sondi B (2004) Silver nanoparticles as antimicrobial agent: a case study on *E. coli* as a model for Gram-negative bacteria. *J Colloid Interface Sci* 275:177–182
- Thomas V, Yallapu MM, Sreedhar B, Bajpai SK (2007) A versatile strategy to fabricate hydrogel–silver nanocomposites and investigation of their antimicrobial activity. *J Colloid Interface Sci* 315:389–395
- Zhao GJ, Stevens SE (1998) Multiple parameters for the comprehensive evaluation of the susceptibility of *Escherichia coli* to the silver ion. *Biometals* 11:27–32